Position-Dependent Diffusion of Light in Disordered Waveguides

Alexey G. Yamilov,[1,*] Raktim Sarma,[2] Brandon Redding,[2] Ben Payne,[1] Heeso Noh,[2,3] and Hui Cao[2,4,†]
[1]Department of Physics, Missouri University of Science and Technology, Rolla, Missouri 65409, USA
[2]Department of Applied Physics, Yale University, New Haven, Connecticut 06520, USA
[3]Department of Nano and Electronic Physics, Kookmin University, Seoul 136-702, Korea
[4]Department of Physics, Yale University, New Haven, Connecticut 06520, USA
(Received 3 August 2013; published 15 January 2014)

We present direct experimental evidence for position-dependent diffusion in open random media. The interference of light in time-reversed paths results in renormalization of the diffusion coefficient, which varies spatially. To probe the wave transport inside the system, we fabricate two-dimensional disordered waveguides and monitor the light intensity from the third dimension. Change the geometry of the system or dissipation limits the size of the loop trajectories, allowing us to control the renormalization of the diffusion coefficient. This work shows the possibility of manipulating wave diffusion via the interplay of localization and dissipation.

DOI: 10.1103/PhysRevLett.112.023904 PACS numbers: 42.25.Dd, 42.25.Bs, 72.15.Rn

As first shown by Einstein in his theory of Brownian motion, the diffusion equation describes the evolution of the density of particles each undergoing a random walk [1]. The power of this approach is that it requires knowledge of a single parameter, D, the diffusion coefficient, regardless of the underlying microscopical mechanisms of transport. If the spatial gradient of the particle density is not too large, the particle flux is linearly proportional to the gradient, and D is the coefficient. Diffusion is also applicable to waves [2], but it ignores interference effects. When inelastic scattering is negligible, most of the elastically scattered waves have uncorrelated phases, and their interference is averaged out. Nevertheless, a wave may return to a position it has previously visited after a random walk, and there always exists the time-reversed path which yields an identical phase delay. Constructive interference of the waves from the reversed loops increases the wave energy density at the original position and decreases the flux, giving the so-called weak localization effect [3]. This is the basic mechanism for the suppression of wave diffusion, which eventually leads to Anderson localization [4,5].

In the self-consistent theory of localization [6,7], the diffusion coefficient D is renormalized, and the amount of renormalization is proportional to the return probability of waves via the looped paths [8]. In an open system of finite size, the return probability is reduced because the longer loops may reach the boundary where waves escape. Thus, the renormalization of D depends on the system size. Moreover, the chance of escape is higher near the boundary where the renormalization of D is weaker. This means that the value of D is no longer constant but varies spatially [9–11]. In the presence of dissipation, the long loops are also cut; thus, the renormalization of the diffusion coefficient depends on the amount of dissipation in both infinite [12] and finite open random media [13]. Furthermore, dissipation introduces a length scale beyond which the wave will not reach the boundary of the system, and the diffusion coefficient becomes position independent [14,15].

Although the self-consistent theory of localization in open random media has been invoked to interpret several experiments [16–18], its key prediction of position-dependent diffusion (PDD) has not been observed directly. This is because it is difficult to probe wave transport inside the system experimentally. In this Letter, we obtain direct experimental evidence of PDD by analyzing the light that escapes from the two-dimensional (2D) random structures via out-of-plane scattering [19–21]. It is well known that the diffusion coefficient can be modified by changing the scattering properties of the random medium. In contrast, we demonstrate that it is possible to change local diffusion without changing the properties of the disorder by varying the geometry of the system or the dissipation (out-of-plane scattering), which also limits the size of the loop trajectories. This is because PDD is caused by the nonlocal wave interference effects that depend on the exact position of the boundary. Our experiment confirms that renormalization of the diffusion coefficient, which has long been considered as a theoretical approach put forward by the self-consistent theory [9,10] and the supersymmetric [11,15] theory to treat localization effects, actually happens inside the random media. It is an intrinsic wave phenomenon that applies not only to electromagnetic waves but also to all other waves such as acoustic waves and matter waves.

We designed and fabricated 2D disordered waveguide structures in a 220 nm silicon layer on top of 3 μm buried oxide. The patterns were written by electron beam lithography and etched in an inductively coupled plasma reactive ion etcher. As shown in the scanning electron microscope (SEM) images in Fig. 1(a), the waveguide has sidewalls made of periodic arrays of air holes. They possess a 2D photonic band gap and provide optical confinement in the plane of the waveguide. Light enters the waveguide from an

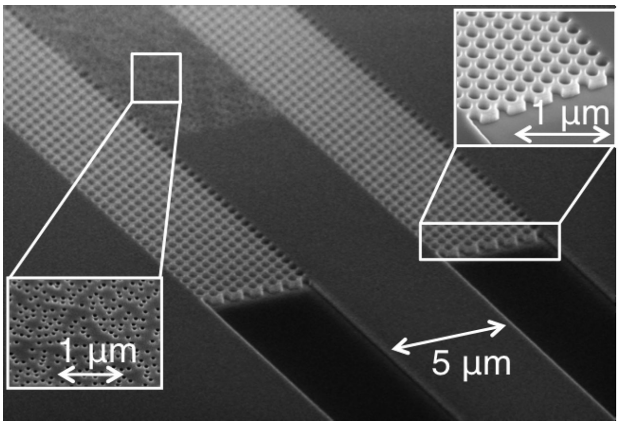

FIG. 1. Tilt-view SEM image of a disordered waveguide fabricated in a silicon membrane on top of silica. The two sidewalls of the waveguide consist of triangular lattices of air holes (lattice constant 440 nm, hole radius 154 nm). They possess a 2D photonic band gap and behave like reflecting walls for light incident from all angles in the waveguide. The probe light (in the wavelength range of 1500–1520 nm) is coupled from a silicon ridge waveguide to an empty photonic crystal waveguide then impinged onto a random array of air holes (hole diameter 100 nm and areal density 6%) inside the waveguide.

open end and is incident onto a 2D array of air holes inside the waveguide [22]. The random pattern of air holes causes light to scatter while going through the waveguide. The transport mean free path ℓ is determined by the size and density of the air holes. Light localization will occur if the length of the random array L exceeds the localization length $\xi = (\pi/2)N\ell$, where $N = 2W/(\lambda/n_e)$ is the number of propagating modes in the waveguide, W is the waveguide width, λ is the optical wavelength in vacuum, and n_e is the effective index of refraction of the random medium. Since N scales linearly with W, ξ can be easily tuned by varying the waveguide width without changing ℓ or n_e. Therefore, by changing the waveguide geometry (L, W), we can reach both the diffusion regime ($\ell < L < \xi$) and the localization regime ($L > \xi$) [23,24]. Although there is no mobility edge [18] in such a system, it is not essential for our goal of observing PDD. The latter is the manifestation of the developing localization effects in the system of finite size L. Because of their reduced dimensionality, the disordered waveguides are always localized in the $L \to \infty$ limit.

In order to apply the self-consistent theory of localization to the analysis of the experimental data below, we first validate it with numerical simulations under conditions close to those in the experiment. In general, the diffusion coefficient D depends not only on the longitudinal coordinate z but also on the transverse coordinate y. For all our samples, we set the waveguide width W much less than the localization length ξ, so that the transverse variation of D can be neglected. Therefore, $D(z)$, which depends only on z, describes the longitudinal evolution of the intensity averaged over the cross section of the waveguide.

We computed the PDD coefficient without making any assumption about the nature or strength of wave interference [22]. Figure 2 plots the calculated $D(z)/D_0$ (the lower dashed line) for $L/\xi = 3.0$, where D_0 is the diffusion coefficient without renormalization. The z axis is parallel to the waveguide, and the random array extends from $z = 0$ to $z = L$. The renormalized $D(z)$ drops to $0.17D_0$ in the middle of the random waveguide ($z = L/2$). Using the self-consistent theory of localization [13], we calculate $D(z)/D_0$ (the lower solid line in Fig. 2), and it is in excellent agreement with the *ab initio* simulation without any fitting parameters. Previous theoretical studies show [13,25] that further into the localization regime where resonant tunneling dominates wave transport, the self-consistent theory of localization underestimates the energy density inside the random system that is strongly affected by the presence of single-localized and necklace states [26]. In our experiment, we keep $L \leq 3\xi$ so that the self-consistent theory of localization holds (as confirmed numerically in Fig. 2).

Another factor we need to consider is the dissipation of light in the random waveguide [27]. The wavelength range of the probe is chosen such that the light absorption by silicon or silica is negligible. Hence, light scattering out of the waveguide plane by the random array of air holes is the dominant loss mechanism. Such scattering allows us to

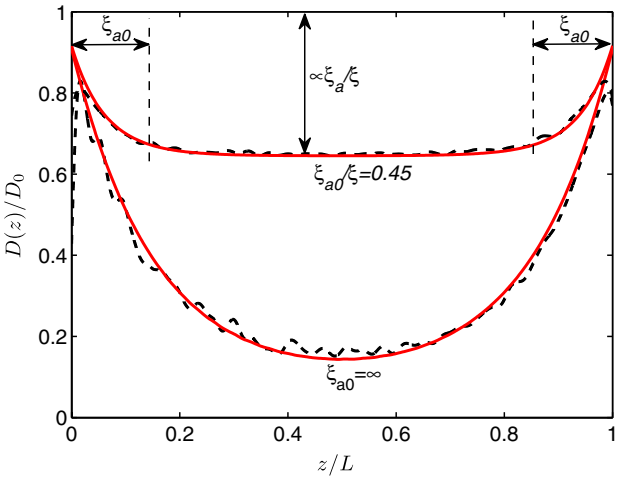

FIG. 2 (color online). Numerically calculated diffusion coefficient $D(z)$ (dashed curves) for $0 < z < L$ in a waveguide filled with randomly positioned scatterers. The waveguide has length $L = 3\xi$ (ξ is the localization length) and supports $N = 10$ modes. The solid curves represent the prediction of the self-consistent theory of localization. D_0 denotes the diffusion coefficient that ignores interference effects. In the absence of dissipation (diffusive dissipation length $\xi_{a0} = \infty$), $D(z)$ drops to a minimum of $0.17D_0$ in the middle of the waveguide. With the addition of dissipation ($\xi_{a0}/\xi = 0.45$), $D(z)$ exhibits a plateau for $\xi_{a0} < z < L - \xi_{a0}$, and its value D_p is determined by the ratio ξ_{a0}/ξ.

study the effect of PDD by monitoring the intensity distribution inside the system from the vertical direction. However, we need to address the question whether the out-of-plane scattering can be treated as incoherent dissipation in our simulations. In a random array of scatterers, the fields are correlated [28,29] only within a distance on the order of one transport mean free path ℓ, and waves from different coherent regions of size $\ell \times \ell$ have uncorrelated phases. Since there is a large number of such coherence regions $\ell \times \ell$ in the random waveguide of size $W \times L$, the overall leakage may be considered incoherent and, thus, treated effectively as material absorption.

To illustrate the effect of dissipation on PDD, we perform numerical simulations. The diffusive dissipation length in the random system is $\xi_{a0} = \sqrt{D_0 \tau_a}$, where τ_a is the ballistic dissipation time. When ξ_{a0} becomes smaller than the localization length ξ, the effect of dissipation is significant. Figure 2 plots the calculated $D(z)/D_0$ in the random waveguide with $\xi_{a0}/\xi = 0.45$ (the upper dashed line) in comparison to that with $\xi_{a0} = \infty$ (no dissipation). The suppression of diffusion is weakened by the dissipation, and a plateau for the renormalized diffusion coefficient is developed inside the disordered system. This result can be understood as follows. Dissipation suppresses the feedback from long propagation paths, limiting the effective size of the system [30] to the order of the diffusive dissipation length for any position that is more than one ξ_{a0} away from the open boundary ($\xi_{a0} < z < L - \xi_{a0}$) [14,15]. Thus, the renormalized D reaches a constant value equal to that of an open system of dimension $\sim 2\xi_a = 2\sqrt{D\tau_a}$. In the remaining regions that are within one ξ_{a0} to the boundary ($z < \xi_{a0}$ and $L - z < \xi_{a0}$), the diffusion coefficient is still position dependent due to leakage through the boundary, and D increases toward the value of D_0. We note that the extent of these regions ξ_{a0} is much greater than the transport mean free path ℓ. The latter determines the boundary region where the diffusion approximation is not accurate even without wave interference [31]. Figure 2 also shows the prediction of the self-consistent theory of localization in the presence of dissipation (the upper solid line), and it agrees well with the numerical result.

The planar waveguide geometry we use is well suited for studying the effect of PDD. It allows a precise fabrication of the desired system using lithography so that the parameters such as the transport mean free path can be accurately controlled. The localization length $\xi \propto W$ can be varied by changing the waveguide width, while the diffusive dissipation length ξ_{a0} remains fixed. This allows us to separate the effects of localization and dissipation by testing waveguides of different width. Unlike 2D random systems [21], the additional confinement of light by the waveguide sidewalls makes ξ scale linearly with ℓ. Even if scattering is relatively weak ($k\ell \gg 1$, where k is the wave number), the waveguide length L can easily exceed ξ so that the localization effect is strong enough to modify the diffusion. Instead of designing the disorder to maximize scattering (minimizing $k\ell$), we deliberately lower the density of the air holes to mitigate the out-of-plane scattering loss and maximize the ratio ξ_{a0}/ξ.

Experimentally, a continuous-wave beam from a wavelength-tunable laser (HP 8168F) was coupled to the waveguide through a single-mode polarization-maintaining lensed fiber. The transverse-electric polarization (electric field in the plane of the waveguide) of the incident light was chosen. A near-field optical image of the spatial distribution of light intensity across the structure surface was taken by collecting light scattered out of plane using a 50X objective lens (numerical aperture 0.42) and recorded by an InGaAs camera (Xenics Xeva 1.7-320) [22]. The intensity was integrated over the cross section of the waveguide to obtain the evolution $I(z)$ along the waveguide (parallel to the z axis). For each configuration (width W, length L, transport mean free path ℓ) of the disordered waveguides, $I(z)$ was averaged over two random realizations of air holes and 50 input wavelengths equally spaced between 1500 and 1520 nm. The wavelength spacing was chosen to produce independent intensity distributions.

Figure 3(a) shows the measured $I(z)$ inside the random waveguides of W varying from 60 to 5 μm (blue solid lines). All other parameters are kept the same, L is fixed at 80 μm, the diameter of the air holes is 100 nm, and the average (center-to-center) distance of the adjacent holes is 390 nm. ℓ and ξ_{a0} are obtained by fitting the least localized sample, $W = 60$ μm (longest ξ), with the self-consistent theory of localization (red dashed line) [22]. We find that $\ell = 2.2 \pm 0.1$ μm and $\xi_{a0} = 30 \pm 0.5$ μm. With the parameters found from the $W = 60$ μm sample, the self-consistent theory of localization successfully predicts the decay for $I(z)$ in all other samples with $W = 40$, 20, 10, 5 μm (red solid lines). We stress that the excellent agreement with the experimental data is obtained without any free parameter except for the vertical intensity scale. The PDD coefficients $D(z)$ corresponding to the red curves in Fig. 3(a) are shown in Fig. 3(b). We can clearly see that the diffusion coefficient is reduced inside the sample, and its value varies along z. Farther away from the open boundary, D has a smaller value. In the narrower waveguides, the reduction of D is larger due to the stronger localization effect. In the most localized sample of $W = 5$ μm, D is reduced to $0.65D_0$ at $z = L/2$. In an attempt to further reduce D, we double the length of the random system L to 160 μm. As shown in Figs. 3(c) and 3(d) for $W = 5$ μm, the minimal D no longer decreases; instead, it saturates in the middle of the random waveguide. This behavior is attributed to dissipation which suppresses localization. As the system length L becomes much larger than the diffusive dissipation length ξ_{a0}, $D(z)$ saturates to a constant value D_p inside the disordered waveguide, similar to the simulation result shown in Fig. 2.

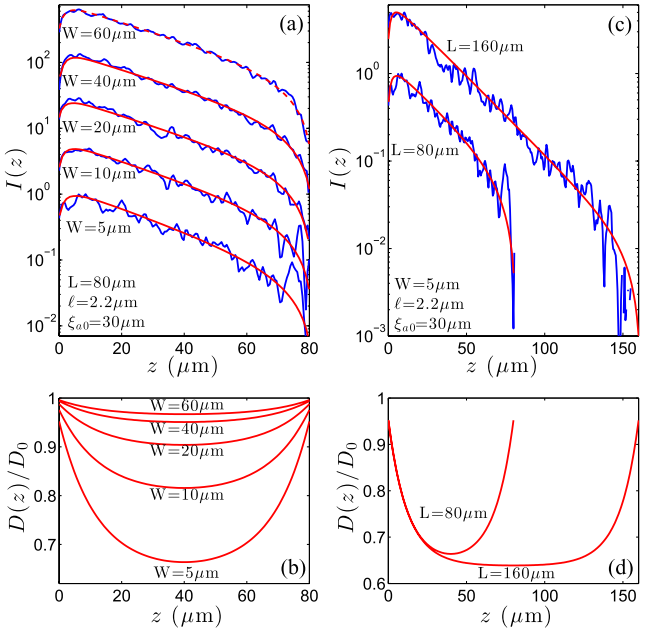

FIG. 3 (color online). (a) Experimentally measured light intensity $I(z)$ inside random waveguides of different width W and constant length $L = 80$ μm (blue solid lines). The curves are vertically shifted for a clear view. $\ell = 2.2$ μm and $\xi_{a0} = 30$ μm are found by fitting the $W = 60$ μm sample with the self-consistent theory of localization (red dashed line). With these parameters, the self-consistent theory of localization predicts $I(z)$ for other samples of $W = 40$, 20, 10, 5 μm (red solid curves), which agrees well with the experimental data. (b) Position-dependent diffusion coefficients for the five samples in (a). (c) Experimentally measured $I(z)$ of two waveguides with the same width $W = 5$ μm but different lengths, $L = 80$, 160 μm (blue solid curves). Red solid curves represent the prediction of the self-consistent theory of localization using the same values of ℓ and ξ_{a0} as in (a). (d) Diffusion coefficients $D(z)$ for the two samples in (c) showing the saturation of D inside the longer sample $L = 160$ μm.

Finally, we exploit the interplay between dissipation and localization to tune the saturated value of the diffusion coefficient inside the random system. To this end, we increase the density of scatterers to reach the deep saturation region $\xi_{a0} \ll L$. In the second set of samples, the diameter of the air holes is 150 nm, and the average distance between the adjacent holes is 370 nm. The waveguide length L is set at 80 μm, and W varies from 5 to 60 μm. The experimental data of the measured intensity $I(z)$ inside the random waveguides are presented in Fig. 4(a). Using the same procedure described earlier, we obtain the values of $D(z)$ shown in Fig. 4(b). Because of stronger scattering (smaller ℓ) and larger out-of-plane loss (shorter ξ_{a0}), $D(z)$ for all five samples displays a well-developed plateau inside the sample. The saturated value of D_p decreases with W—the narrower waveguide has a smaller D_p. Hence, without changing the disorder or altering the dissipation rate, we can control the diffusion inside a random system by merely varying its geometry (W, in this case).

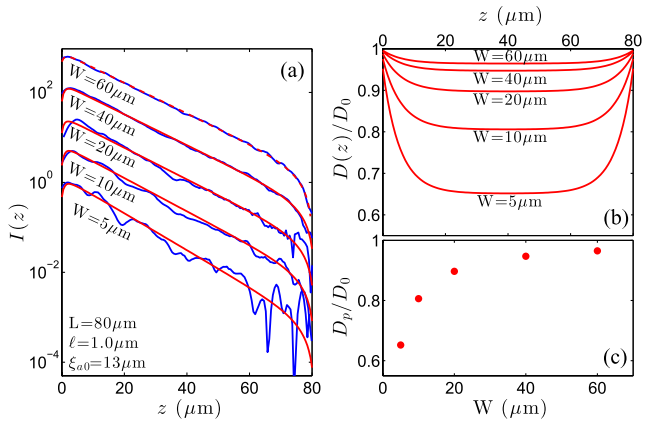

FIG. 4 (color online). Tuning the diffusion coefficient via the interplay of localization and dissipation. (a) Experimentally measured light intensity $I(z)$ inside random waveguides in the deep saturation regime $\xi_{a0} \ll L$ (blue solid lines). The curves are vertically offset for a clear view. The length and width of the waveguides are given in the graph. $\ell = 1.0$ μm and $\xi_{a0} = 13$ μm are found by fitting the $W = 60$ μm sample with the self-consistent theory of localization (red dashed line). These values are then used to predict $I(z)$ for other samples $W = 40$, 20, 10, 5 μm (red solid curves), which is in good agreement with the experimental data with no fitting parameters except the vertical intensity scale. (b) Diffusion coefficients $D(z)$ for all samples in (a) are saturated in the region $\xi_{a0} < z < L - \xi_{a0}$. (c) The saturated value of the diffusion coefficient D_p from (b) uniformly decreases with the decrease of the waveguide width.

In summary, we presented the direct experimental evidence of position-dependent suppressed diffusion of light inside the random systems. By varying the size and shape of the random system, we were able to manipulate the degree of renormalization of D. We also showed that the presence of dissipation prevents D from approaching zero and sets a limit for the minimal value of the renormalized diffusion constant that can be reached by the localization corrections. Such effect of dissipation is expected to be similar to that of dephasing in the electronic systems [32].

We are indebted to Patrick Sebbah and Shivakiran Bhaktha for their insight in selecting the experimental geometry. We acknowledge Seng Fatt Liew, Douglas Stone, Arthur Goetschy, Boris Shapiro, and Sergey Skipetrov for useful discussions. We also thank Michael Rooks for suggestions regarding sample fabrication. This work was supported by the National Science Foundation under Grants No. DMR-1205307, No. DMR-1205223, and No. ECCS-1128542. Computational resources were provided under the Extreme Science and Engineering Discovery Environment (XSEDE) Grant No. DMR-100030. Facilities use was supported by YINQE and NSF MRSEC Grant No. DMR-1119826.

*yamilov@mst.edu
†hui.cao@yale.edu

[1] A. Einstein, Ann. Phys. (Berlin) **322**, 549 (1905).
[2] A. Ishimaru, *Wave Propagation and Scattering in Random Media* (Academic Press, New York, 1978).
[3] L. Gor'kov, A. Larkin, and D. Khmel'nitskii, JETP Lett. **30**, 228 (1979).
[4] P. W. Anderson, Phys. Rev. **109**, 1492 (1958).
[5] A. Lagendijk, B. van Tiggelen, and D. S. Wiersma, Phys. Today **62**, No. 8, 24 (2009).
[6] D. Vollhardt and P. Wölfle, Phys. Rev. B **22**, 4666 (1980).
[7] J. Kroha, C. M. Soukoulis, and P. Wölfle, Phys. Rev. B **47**, 11093 (1993).
[8] S. Hikami, Phys. Rev. B **24**, 2671 (1981).
[9] B. A. van Tiggelen, A. Lagendijk, and D. S. Wiersma, Phys. Rev. Lett. **84**, 4333 (2000).
[10] N. Cherroret and S. E. Skipetrov, Phys. Rev. E **77**, 046608 (2008).
[11] C. Tian, Phys. Rev. B **77**, 064205 (2008).
[12] R. Frank, A. Lubatsch, and J. Kroha, Phys. Rev. B **73**, 245107 (2006).
[13] B. Payne, A. Yamilov, and S. E. Skipetrov, Phys. Rev. B **82**, 024205 (2010).
[14] A. Yamilov and B. Payne, Opt. Express **21**, 11688 (2013).
[15] L. Y. Zhao, C. S. Tian, Z. Q. Zhang, and X. D. Zhang, Phys. Rev. B **88**, 155104 (2013).
[16] M. Störzer, P. Gross, C. M. Aegerter, and G. Maret, Phys. Rev. Lett. **96**, 063904 (2006).
[17] H. Hu, A. Strybulevych, J. H. Page, S. E. Skipetrov, and B. A. van Tiggelen, Nat. Phys. **4**, 945 (2008).
[18] T. Sperling, W. Bührer, C. M. Aegerter, and G. Maret, Nat. Photonics **7**, 48 (2012).
[19] J. Topolancik, B. Ilic, and F. Vollmer, Phys. Rev. Lett. **99**, 253901 (2007).
[20] L. Sapienza, H. Thyrrestrup, S. Stobbe, P. D. Garcia, S. Smolka, and P. Lodahl, Science **327**, 1352 (2010).
[21] F. Riboli, P. Barthelemy, S. Vignolini, F. Intonti, A. D. Rossi, S. Combrie, and D. S. Wiersma, Opt. Lett. **36**, 127 (2011).
[22] See Supplemental Material at http://link.aps.org/supplemental/10.1103/PhysRevLett.112.023904 for description of the optical measurement setup and numerical calculation of position dependent diffusion coefficient.
[23] D. J. Thouless, Phys. Rev. Lett. **39**, 1167 (1977).
[24] A. Z. Genack and A. A. Chabanov, J. Phys. A **38**, 10465 (2005).
[25] C. S. Tian, S. K. Cheung, and Z. Q. Zhang, Phys. Rev. Lett. **105**, 263905 (2010).
[26] J. B. Pendry, J. Phys. C **20**, 733 (1987).
[27] A. A. Chabanov, M. Stoytchev, and A. Z. Genack, Nature (London) **404**, 850 (2000).
[28] B. Shapiro, Phys. Rev. Lett. **57**, 2168 (1986).
[29] S. Feng, C. Kane, P. A. Lee, and A. D. Stone, Phys. Rev. Lett. **61**, 834 (1988).
[30] P. W. Brouwer, Phys. Rev. B **57**, 10526 (1998).
[31] E. Akkermans and G. Montambaux, *Mesoscopic Physics of Electrons and Photons* (Cambridge University Press, Cambridge, England, 2007), ISBN 0-521-85512-8.
[32] *Mesoscopic Phenomena in Solids*, edited by B. L. Altshuler, P. A. Lee, and R. A. Webb (North Holland, Amsterdam, 1991).

SUPPLEMENTAL MATERIAL
Position-dependent diffusion of light in disordered waveguides

Alexey G. Yamilov[1*], Raktim Sarma[2], Brandon Redding[2], Ben Payne[1], Heeso Noh[2,3] & Hui Cao[2,4†]
[1]*Department of Physics, Missouri University of Science & Technology, Rolla, Missouri 65409, USA*
[2]*Department of Applied Physics, Yale University, New Haven, Connecticut 06520, USA*
[3]*Department of Nano and Electronic Physics, Kookmin University, Seoul 136-702, Korea*
[4]*Department of Physics, Yale University, New Haven, Connecticut 06520, USA*

PACS numbers: 42.25.Dd,42.25.Bs,72.15.Rn

MAPPING FROM 3D TO 2D WAVE EQUATION

The random waveguide, c.f. Fig. [1] in the main text, is made of perforated silicon membrane, sandwiched between air and silica. The dielectric constant of this 3D system is $\epsilon(x,y,z) = [n(x,y,z)]^2$, and the wave equation is

$$\left\{\nabla^2_{3D} + [kn(x,y,z)]^2\right\} E(x,y,z) = 0. \qquad (1)$$

The transformation of the above wave equation to 2D wave equation involves two assumptions – effective index and effective absorption approximations.

Because the refractive index $n(x,y,z)$ of our system is not factorizable, the above wave equation does not separate exactly into a normal (x-axis) and in-plane (y,z-axes) equations. The transformation from the 3D wave equation to a 2D wave equation for y,z coordinates is known as effective index approximation. This involves replacing $n(x,y,z)$ by an effective index $\tilde{n}$ that depends only on y,z. The 2D wave equation is

$$\left\{\nabla^2_{2D} + [k\tilde{n}(y,z)]^2\right\} \tilde{E}(y,z) = 0. \qquad (2)$$

The value of $\tilde{n}(y,z)$ is chosen to be one within the air holes and n_d in the dielectric. The value of n_d can be found from a procedure described e.g. in Ref. [1]. The most important limitations of this approach are:
(i) $\tilde{n}$ varies with frequency even if $n(x,y,z)$ is independent of frequency;
(ii) $\tilde{n}$ is a real number and it does not account for the out-of-plane leakage of light from the membrane.

(i) is not an issue in our experiments using continuous-wave monochromatic light.

(ii) can be mitigated with another approximation: the out-of-plane scattering loss can be accounted for by adding an imaginary part to the effective dielectric constant, $\tilde{\epsilon}(y,z) = (1+i\alpha)[\tilde{n}(y,z)]^2$, where α is the effective absorption coefficient. For a periodically perforated membrane, the effective absorption is not always justified because the out-of-plane loss, unlike the absorption, can be a non-local process. This is because long-range correlation of light fields in a periodic array of scatterers makes the waves scattered from different locations phase coherent and they interfere in the far field. However, in a random array of scatterers, the fields are correlated only within a distance of the order one transport mean free path ℓ [2, 3], and waves from different coherent regions $\ell \times \ell$ have uncorrelated phases. Since there are a large number of such coherence regions $\ell \times \ell$ in our waveguides $W \times L$, the overall leakage may be considered incoherent and treated effectively as absorption.

CALCULATION OF POSITION-DEPENDENT DIFFUSION COEFFICIENT $D(z)$

In the ab-initio numerical simulation, we consider a monochromatic scalar wave $E(\mathbf{r})e^{-i\omega t}$ propagating in a 2D volume-disordered waveguide of width W and length $L \gg W$. The wave field $E(\mathbf{r})$ obeys the 2D Helmholtz equation:

$$\left\{\nabla^2 + k^2\left[1 + \delta\epsilon(\mathbf{r})\right]\right\} E(\mathbf{r}) = 0. \qquad (3)$$

Here $k = \omega/c$ is the wavenumber and $\delta\epsilon(\mathbf{r}) = (1 + i\alpha)\delta\epsilon_r(\mathbf{r})$, where $\delta\epsilon_r(\mathbf{r})$ describes the random fluctuation of the dielectric constant, and $\alpha > 0$ denotes the strength of dissipation. The system is excited from one open end ($z = 0$) of the waveguide (extending from $z = 0$ to $z = L$) by illuminating each of the guided modes with a unit flux. The wave field $E(\mathbf{r})$ throughout the random medium is computed with the transfer matrix method for a given realization of disorder[4]. From $E(\mathbf{r})$ we calculate the energy density $\mathcal{W}(z)$ and the flux $J_z(z)$ along the z axis (parallel to the waveguide axis). These two quantities are averaged over the cross section of the waveguide at each z and give the diffusion coefficient:

$$D(z) = -\langle J_z(z)\rangle / \left[d\langle \mathcal{W}(z)\rangle/dz\right], \qquad (4)$$

where the averages $\langle \ldots \rangle$ are taken over a statistical ensemble of 10^6 disorder realizations.

In order to compare our numerical results for $D(z)$ with the self-consistent theory of localization, we need to have

*e-mail:yamilov@mst.edu
†e-mail:hui.cao@yale.edu

the value of the diffusion coefficient without renormalization due to the wave interference effects $D_0 = v\ell/2$. To estimate the transport mean free path ℓ in our model we perform a set of simulations for different waveguide lengths L, exploring both the regime of diffusion $L < \xi$ and that of Anderson localization $L > \xi$. We computed numerically the conductance g as the sum of transmission coefficients from all incoming to all outgoing waveguide modes. The dependencies of the average $\langle g \rangle$ and variance $\mathrm{var}(g)$ on L are fitted by the analytical expressions obtained by Mirlin in Ref. [5] using the supersymmetry approach with ℓ being the only fit parameter. To find the diffusive speed v, we use the definition of diffusive flux in the forward $(+z)$ direction $J_z^{(+)}(z)$ and the backward $(-z)$ direction $J_z^{(-)}(z)$ with respect to the propagation direction[6]

$$\langle J_z^{(\pm)}(z)\rangle = (v/\pi)\langle \mathcal{W}(z)\rangle \mp (D(z)/2)d\langle \mathcal{W}(z)\rangle/dz. \quad (5)$$

Combining the two components, we find the diffusive speed

$$v = 2\left(\langle J_z^{(+)}(z)\rangle + \langle J_z^{(-)}(z)\rangle\right)/\langle \mathcal{W}(z)\rangle. \quad (6)$$

Dashed lines in Fig. 1 depict $D(z)$ found in equation (4) normalized by D_0.

In the dissipative random waveguides, the characteristic dissipation time τ_a is determined numerically using the condition of flux continuity $d\langle J_z(z)\rangle/dz = (1/\tau_a)\langle \mathcal{W}(z)\rangle$. The desired diffusive dissipation length $\xi_{a0} = \sqrt{D_0\tau_a}$ can be obtained by the proper choice of α in equation (3).

SELF-CONSISTENT THEORY OF LOCALIZATION

The self-consistent theory starts with the Green's function $G(\mathbf{r},\mathbf{r}')$ of equation (3) with $\delta\epsilon(\mathbf{r}) = \delta\epsilon_r(\mathbf{r}) + i\alpha$. In a random waveguide, the disorder-averaged function $\hat{C}(\mathbf{r},\mathbf{r}') = (4\pi W D_0/cL)\langle |G(\mathbf{r},\mathbf{r}')|^2\rangle$ obeys self-consistent equations in a dimensionless form[4, 7]:

$$\left[\left(\frac{L}{\xi_{a0}}\right)^2 - \frac{\partial}{\partial\zeta}d(\zeta)\frac{\partial}{\partial\zeta}\right]\hat{C}(\zeta,\zeta') = \delta(\zeta-\zeta'), \quad (7)$$

$$\frac{1}{d(\zeta)} = 1 + \frac{2L}{\xi}\hat{C}(\zeta,\zeta), \quad (8)$$

where $d(\zeta) = D(\zeta)/D_0$ and all position-dependent quantities are functions of the longitudinal coordinate $\zeta = z/L$. The quantity $\hat{C}(\zeta,\zeta)$, which renormalizes the diffusion coefficient, is proportional to the return probability at ζ. Assuming first that $d(\zeta) \equiv 1$, equations (7,8) are solved by iteration with the boundary conditions:

$$\hat{C}(\zeta,\zeta') \mp \frac{z_0}{L}d(\zeta)\frac{\partial}{\partial\zeta}\hat{C}(\zeta,\zeta') = 0 \quad (9)$$

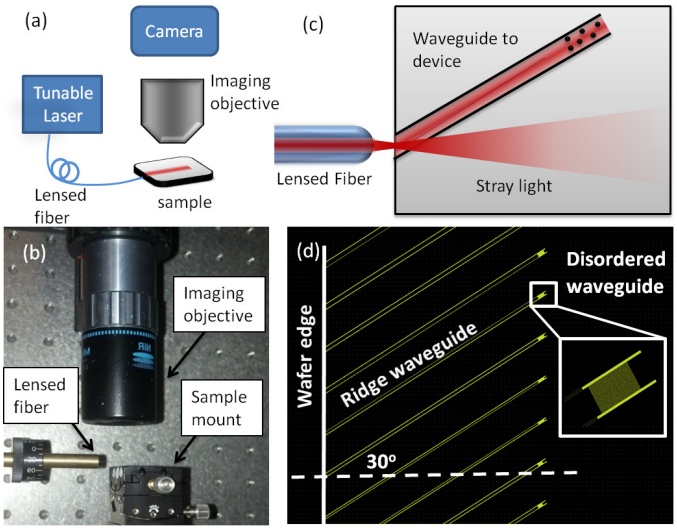

Figure S 1: Optical measurement setup: (a) Schematic of experimental setup for measuring light transport inside the random waveguide. (b) Photograph of the experimental setup. (c) Schematic of the sample layout showing the ridge waveguides coupling the probe light from the edge of the wafer to the random waveguides with photonic crystal sidewalls. (d) Layout of the fabricated structures studied experimentally.

at $\zeta = 0$ and $\zeta = 1$. The $z_0 = (\pi/4)\ell$ is the so-called extrapolation length[6].

After the self-consistent solution of equations (7-9) has been found, we find the intensity distribution inside the sample by replacing the delta-function source in equation (7) with $(L/\ell)\exp[-\zeta/(\ell/L)]$. This source term represents the exponential attenuation of the incident ballistic signal.

EXPERIMENTAL DETAILS

Optical measurement setup: The experimental setup for optical characterization is shown in Fig. S1(a). We used a single-mode polarization-maintaining fiber to deliver the probe light into a silicon ridge waveguide on a SOI substrate. The fiber was tapered at the end to focus the laser beam to a spot of diameter ~ 2.5 μm at the edge of the wafer. The ridge waveguide had the same width as the random waveguide it was connected to, which varied from 5 micron to 60 micron [Fig. S1(b)]. However, the height of the silicon waveguide was merely 220 nm, so some of the input light did not couple into the waveguide; instead it propagated above or below the waveguide. To avoid such stray light, the ridge waveguide was tilted by 30 degrees with respect to the incident direction of the light from the fiber (approximately normal to the edge of the wafer). The ridge waveguide was made 2.5 mm long, so that the random waveguide structure is far from

the direct path of the stray light. In addition, uniform illumination of the front surface of the random structure inside the waveguide was ensured by positioning the tapered fiber approximately at the center of the input facet of the ridge waveguide. The spatial distribution of light intensity over the sample was imaged by an objective lens onto an IR CCD camera [not shown in Fig. S1(a)].

Design of photonic crystal walls for 2D waveguides: The triangular lattice of air holes that form the sidewalls of the random waveguide were designed to have a 2D photonic bandgap for TE polarized light in the wavelength range of 1450 nm – 1550 nm. The photonic band structure was calculated with the plane wave expansion method[8].

[1] M. Hammer and O. Ivanova, Opt. Quantum Electr. **41**, 267 (2009).

[2] B. Shapiro, Phys. Rev. Lett. **57**, 2168 (1986).

[3] S. Feng, C. Kane, P. A. Lee, and A. D. Stone, Phys. Rev. Lett. **61**, 834 (1988).

[4] B. Payne, A. Yamilov, and S. E. Skipetrov, Phys. Rev. B **82**, 024205 (2010).

[5] A. Mirlin, Phys. Rep. **326**, 259 (2000).

[6] M. C. van Rossum and T. M. Nieuwenhuizen, Rev. Mod. Phys. **71**, 313 (1999).

[7] N. Cherroret and S. E. Skipetrov, Phys. Rev. E **77**, 046608 (2008).

[8] S. G. Johnson and J. D. Joannopoulos, Opt. Express **8**, 173 (2001).